Data in Brief 32 (2020) 106208

Contents lists available at ScienceDirect

Data in Brief

journal homepage: www.elsevier.com/locate/dib

Data Article

Simulated infrared and Raman spectroscopy, complex dielectric function and refractive index dataset of monoclinic *C*2/*m* stoichiometric clinochlore $Mg_6Si_4O_{10}(OH)_8$ as obtained from Density Functional Theory

Gianfranco Ulian, Daniele Moro, Giovanni Valdrè*

Dipartimento di Scienze Biologiche, Geologiche e Ambientali, Centro di Ricerche Interdisciplinari di Biomineralogia, Cristallografia e Biomateriali, Università di Bologna "Alma Mater Studiorum" Piazza di Porta San Donato 1, 40126 Bologna, Italy

ARTICLE INFO

Article history:
Received 30 July 2020
Revised 6 August 2020
Accepted 18 August 2020
Available online 22 August 2020

Keywords:
Clinochlore
Georesources
Phyllosilicates
Infrared spectroscopy
Raman spectroscopy
Dielectric function
Complex refractive index
DFT

ABSTRACT

This article reports a simulated dataset of the vibrational (infrared and Raman) and optical properties (complex dielectric function and refractive index) of clinochlore, an important mineral belonging to the phyllosilicate family [1]. The data here reported were calculated from *ab initio* Density Functional Theory (DFT) simulations at B3LYP level, including a correction for the dispersive forces (B3LYP-D* approach) and all-electron Gaussian-type orbitals basis sets. This dataset was calculated between 0 cm^{-1} and 4000 cm^{-1} and comprises infrared, reflectance and Raman spectra, frequency-dependent complex dielectric function and complex refractive index of clinochlore. The data was validated against available experimental spectroscopic results reported in literature and can be of help in several application fields, for instance fundamental georesource exploration and exploitation, in applied mineralogy, geology, material science, and as a reference to assess the quality of other theoretical approaches.

DOI of original article: 10.1016/j.clay.2020.105779
* Corresponding author.
E-mail address: giovanni.valdre@unibo.it (G. Valdrè).

https://doi.org/10.1016/j.dib.2020.106208

Specifications Table

Subject	Material Science
Specific subject area	Infrared and Raman spectroscopy data of georesouces raw minerals
Type of data	Table Graph Figure
How data were acquired	Quantum mechanical simulations at the DFT/B3LYP-D* level of theory (CRYSTAL17 code)
Data format	Raw Analyzed
Parameters for data collection	Infrared spectra were calculated using adsorption formulas related to the complex dielectric function of the mineral. The spectra were obtained in the range 0 – 4000 cm^{-1} (step of 1 cm^{-1}) and smoothed with a damping factor of 8 cm^{-1}. Raman spectra were simulated considering a 532 nm laser source at 298 K.
Description of data collection	The data were obtained from quantum mechanical simulations conducted using Density Functional Theory, B3LYP functional and Gaussian-type orbitals basis sets. A correction for the dispersive forces based on the DFT-D2 method was also employed (B3LYP-D* scheme).
Data source location	The quantum mechanical simulations were conducted at the University of Bologna, Dept. Biological, Geological and Environmental Sciences, Bologna, Italy.
Data accessibility	With the article
Related research articles	Ulian, G., Moro, D. & Valdrè, G. (2020) Infrared and Raman spectroscopic features of Clinochlore $Mg_6Si_4O_{10}(OH)_8$: a Density Functional Theory contribution. Applied Clay Science, DOI https://doi.org/10.1016/j.clay.2020.105779.

Value of the Data

- The present extensive dataset on the infrared and Raman spectroscopic features of monoclinic stoichiometric clinochlore of composition $Mg_6Si_4O_{10}(OH)_8$ represents a foundation for future fundamental and applied studies on this mineral and related phases.
- Raman and infrared spectroscopies are key investigation techniques to characterize clay mineral georesources and the present dataset provides fundamental insights and procedures to characterize for what concerns Raman and IR complex clay mineral phase composed of brucitic and talc-like layers.
- The present dataset could be used for direct comparison with other experimental and/or theoretical studies.
- Optical properties of clinochlore (complex dielectric function and complex refractive index) could be useful for specific developments of tailored materials with desired optical responses.

1. Data Description

Clinochlore [$Mg_6Si_4O_{10}(OH)_8$] is a phyllosilicate mineral belonging to the chlorite group, composed by alternately stacked brucite-like sheets [$Mg(OH)_2$, labelled as O'] and talc-like ($Mg_3Si_4O_{10}(OH)_2$, TOT) layers. The different layered structures are held together by weak interactions (mainly hydrogen bonds). Stoichiometric clinochlore belongs to the $C2/m$ space group, with lattice parameters $a = 5.3297$ Å, $b = 9.2309$ Å, $c = 14.8947$ Å, $\alpha = \gamma = 90°$ and $\beta = 96.829°$, as obtained from Density Functional Theory (DFT) structural optimization [1].

Data of vibrational (infrared and Raman) properties of clinochlore in the range 0 – 4000 cm^{-1} were obtained at Γ point by Density Functional Theory simulations. Other optical properties

were evaluated in order to obtain the mentioned infrared and Raman data, in particular the frequency-dependent complex dielectric function ($\varepsilon(\omega) = \varepsilon_1(\omega) + \varepsilon_2(\omega)$, with $\varepsilon_1(\omega)$ and $\varepsilon_2(\omega)$ the real and imaginary parts, respectively) and the complex refractive index ($\bar{n} = n + ik$, with n the phase velocity and k the extinction coefficient).

The related datasets are reported in tabular form in Supplementary Material:

- the complex dielectric function, calculated over the *xx, yy* and *zz* directions, which was employed to obtain the IR absorbance, is presented in Table S1 (Supplementary Material);
- the infrared absorption and reflectance spectra, calculated using different approximations (see below), are reported in Table S2 (Supplementary Material);
- the Raman spectra, obtained considering the mineral either as a polycrystalline aggregate and as single crystal, are reported in Table S3 (Supplementary Material);
- the complex refractive index $\bar{n} = n + ik$, calculated over the *xx, yy* and *zz* directions, is presented in Table S4 (Supplementary Material).

These datasets could be of use for comparisons with both experimental and theoretical researches. To cite an example, Fig. 1 reports some of the calculated data at the DFT/B3LYP-D* level of theory.

2. Experimental Design, Materials and Methods

The data here presented were obtained from Density Functional Theory simulations performed with the CRYSTAL17 code [2].

The basis sets describing clinochlore were obtained from linear combination of atomic orbitals (LCAO), the latter being Gaussian-type functions (GTF). More into details, the atomic basis sets for silicon, magnesium, oxygen and hydrogen were 88-31G*, 8-511d1G, 8-411d11G and 3-1p1G, respectively [1, 3].

The hybrid B3LYP functional [4, 5], which is well-known for its ability to produce high quality data for different properties of crystalline systems [6–8], has been adopted for all calculations. The effect of weak interactions on both structural and vibrational data was included with the DFT-D2 correction scheme as modified for the B3LYP functional (B3LYP-D* approach) [9]. This is a necessary correction to the total energy of the system, because both standard and hybrid DFT functionals do not provide an adequate description of dispersive forces that play a major role in layered materials such as phyllosilicates. The exchange and correlation contributions to the total energy were evaluated on a grid made of 75 points and 974 angular points, obtained according to the Gauss–Legendre quadrature and Lebedev schemes. The tolerance thresholds that control accuracy of the Coulomb and exchange integrals were set to 10^{-7} and 10^{-16}, respectively [2]. A $6 \times 6 \times 2$ Monkhorst-Pack grid (26 k-points in the first Brillouin zone) was employed to diagonalize the Hamiltonian matrix. The convergence on total energy was reached when the difference between the energy of two subsequent self-consistent field cycles was less than 10^{-8} Hartree during geometry optimization and less than 10^{-10} Hartree during phonon calculations. Stricter convergence criteria are needed for vibrational properties, as they are obtained from numerical differentiation (dynamic matrix / forces calculation) [10].

The Γ-point vibrational frequencies were calculated by diagonalizing the mass-weighted Hessian matrix, whose elements are the second derivatives of the lattice potential with respect to mass-weighted atomic displacements as explained by Pascale and co-workers [10].

The infrared spectrum of clinochlore was analytically calculated using different adsorption formulas, as described by Maschio and co-workers [11]. More into details, the infrared absorption is calculated using the complex dielectric function $\varepsilon(\nu)$ (dielectric permittivity), which is obtained from, for each inequivalent polarization direction, the Drude-Lorentz model:

$$\varepsilon_{ii}(\nu) = \varepsilon_{\infty,ii} + \sum_p \frac{f_{p,ii}\nu_p^2}{\nu_p^2 - \nu^2 - i\nu\gamma_p} \quad (1)$$

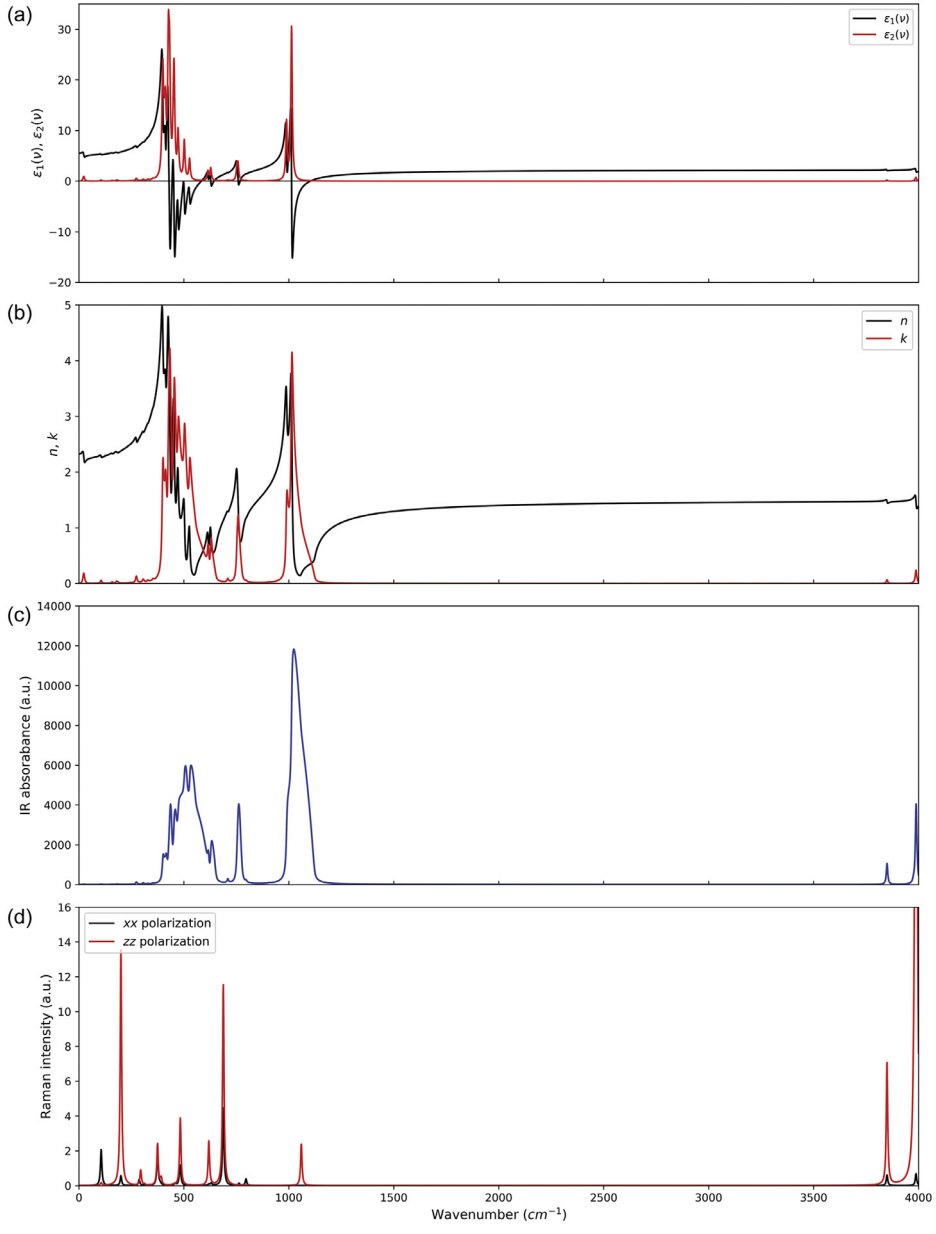

Fig. 1. (a) real (ε_1) and imaginary (ε_2) parts of the dielectric function, (b) complex refractive index, (c) infrared spectrum according to the classical absorption formula [Eq. (5), *vide infra*] and (d) *xx*- and *zz*-polarized Raman spectra of clinochlore, all in the range 0 – 4000 cm^{-1}. The complex dielectric function (a) and the complex refractive index (b) were plotted as averages over all the polarization directions.

with *ii* indicating the polarization direction, ε_∞ is the optical dielectric tensor, ν_p, f_p and γ_p are the (transverse optical) vibrational frequency, the oscillator strength and the damping factor for the *p*-th vibrational mode. Both real and imaginary parts of the dielectric function, $Re[\varepsilon(\nu)]$ and $Im[\varepsilon(\nu)]$, respectively, were computed.

The complex refractive index, $\bar{n} = n + ik$, with n the phase velocity and k the extinction coefficient was calculated according to the following relations:

$$n_{ii}^2(\nu) - k_{ii}^2(\nu) = Re[\varepsilon_{ii}(\nu)] \quad 2n_{ii}(\nu)k_{ii}(\nu) = Im[\varepsilon_{ii}(\nu)] \tag{2}$$

The reflectance spectrum, $R_{ii}(\nu)$, is calculated for each inequivalent direction *ii* as:

$$R_{ii}(\nu) = \left| \frac{\sqrt{\varepsilon_{ii}(\nu) - sin^2(\theta)} - cos(\theta)}{\sqrt{\varepsilon_{ii}(\nu) - sin^2(\theta)} + cos(\theta)} \right|^2 \tag{3}$$

with θ the incidence angle of the beam with respect to the normal to the crystal surface. For the calculations related to the present dataset, this angle was set to 10°.

The infrared absorbance spectrum, $A(\nu)$, was then calculated according to four different models. In the first one, the only one not requiring the complex dielectric function, the IR absorbance was obtained by raw superposition of Lorentzian peaks according to the formula:

$$A_{Lorentzian}(\nu) = \sum_p \frac{I_p}{\pi} \frac{\gamma_p/2}{(\nu - \nu_p)^2 - \gamma_p^2/4} \tag{4}$$

The second model is a classical absorption formula, averaged over the polarization direction *xx*, *yy* and *zz* (1, 2 and 3, according to the Voigt's notation):

$$A_{classical}(\nu) = \frac{1}{3} \sum_{ii=1}^{3} \frac{4\pi}{\lambda\rho} k_{ii}(\nu) \tag{5}$$

with λ the wavelength of the incident beam and ρ the mineral density.

The third and fourth formulas involves Rayleigh approximation of particles having spherical shape and as continuous distribution of ellipsoids, respectively:

$$A_{spherical}(\nu) = \frac{1}{3} \sum_{ii=1}^{3} \frac{2\pi}{\lambda\rho} Im\left[\frac{\varepsilon_{ii}(\nu) - 1}{\varepsilon_{ii}(\nu) + 2}\right] \tag{6}$$

$$A_{ellipsoidal}(\nu) = \frac{1}{3} \sum_{ii=1}^{3} \frac{2\pi}{\lambda\rho} Im\left[\frac{2\varepsilon_{ii}(\nu)}{\varepsilon_{ii}(\nu) - 1} \log \varepsilon_{ii}(\nu)\right] \tag{7}$$

The Raman spectra were calculated by considering the mineral both as a polycrystalline powder and as a single-crystal. Their construction is based on the transverse optical vibrational modes of clinochlore that uses a pseudo-Voigt functional form [12, 13]:

$$A(\nu) = \eta L(\nu) + (1 - \eta) G(\nu) \tag{8}$$

In Eq. (8), $A(\nu)$ is the Raman intensity, $L(\nu)$ is a Lorentzian function with formula given by Eq. (4), η is the Lorentzian factor and $G(\nu)$ is a Gaussian function given by:

$$G(\nu) = \sum_p 2\sqrt{\frac{\ln 2}{\pi}} \frac{I_p}{\gamma_p} exp\left[-\frac{4 \ln 2 (\nu - \nu_p)^2}{\gamma_p^2}\right] \tag{9}$$

with I_p the computed Raman intensities for the p^{th} vibrational mode.

All of the above optical and vibrational quantities were calculated in the spectral range 0 – 4000 cm^{-1}. The optical dielectric tensor, ε_∞, was computed using a couple-perturbed Kohn-Sham approach [14, 15]. The damping factor represents the full width at half maximum of each vibrational mode and was set to 8 for both infrared and Raman spectra because this value provides band broadening similar to that of experimental samples and is also the default employed by CRYSTAL, as described by Maschio and co-workers [11]. Raman spectra were simulated using a pure Lorentzian form, which is the default of CRYSTAL [12], corresponding to $\eta = 1$, to obtain the typical sharp peaks of Raman spectra [16]. Also, the Raman intensities were calculated considering a 532 nm laser source at 298 K.

Declaration of Competing Interest

The authors declare that they have no known competing financial interests or personal relationships which have, or could be perceived to have, influenced the work reported in this article.

Acknowledgments

This research did not receive any specific grant from funding agencies in the public, commercial, or not-for-profit sectors.

Supplementary Materials

Supplementary material associated with this article can be found in the online version at doi:10.1016/j.dib.2020.106208.

References

[1] G. Ulian, D. Moro, G. Valdrè, Infrared and Raman spectroscopic features of Clinochlore $Mg_6Si_4O_{10}(OH)_8$: a Density Functional Theory contribution, Appl. Clay Sci. (2020) in press, doi:10.1016/j.clay.2020.105779.
[2] R. Dovesi, V.R. Saunders, C. Roetti, R. Orlando, C.M. Zicovich-Wilson, F. Pascale, B. Civalleri, K. Doll, N.M. Harrison, I.J. Bush, P. D'Arco, M. Llunell, M. Causà, Y. Noel, L. Maschio, A. Erba, M. Rerat, S. Casassa, CRYSTAL17 User's Manual, University of Torino, Torino, 2017.
[3] D. Moro, G. Ulian, G. Valdrè, Amino acids-clay interaction at the nano-atomic scale: the L-alanine-chlorite system, Appl. Clay Sci. 172 (2019) 28–39.
[4] A.D. Becke, Density-functional thermochemistry.3. The role of exact exchange, J. Chem. Phys. 98 (1993) 5648–5652.
[5] C.T. Lee, W.T. Yang, R.G. Parr, Development of the Colle-Salvetti correlation-energy formula into a functional of the electron-density, Phys. Rev. B 37 (1988) 785–789.
[6] G. Ulian, G. Valdrè, Effects of fluorine content on the elastic behavior of topaz Al2SiO4(F,OH)(2), Am. Mineral. 102 (2017) 347–356.
[7] G. Ulian, D. Moro, G. Valdrè, First principle investigation of the mechanical properties of natural layered nanocomposite: Clinochlore as a model system for heterodesmic structures, Compos. Struct 202 (2018) 551–558.
[8] G. Ulian, G. Valdrè, Structural, vibrational and thermophysical properties of pyrophyllite by semi-empirical density functional modelling, Phys. Chem. Miner. 42 (2015) 609–627.
[9] B. Civalleri, C.M. Zicovich-Wilson, L. Valenzano, P. Ugliengo, B3LYP augmented with an empirical dispersion term (B3LYP-D*) as applied to molecular crystals, CrystEngComm 10 (2008) 405–410.
[10] F. Pascale, C.M. Zicovich-Wilson, F.L. Gejo, B. Civalleri, R. Orlando, R. Dovesi, The calculation of the vibrational frequencies of crystalline compounds and its implementation in the CRYSTAL code, J. Comput. Chem. 25 (2004) 888–897.
[11] L. Maschio, B. Kirtman, R. Orlando, M. Rerat, Ab initio analytical infrared intensities for periodic systems through a coupled perturbed Hartree-Fock/Kohn-Sham method, J. Chem. Phys. 137 (2012) 204113.
[12] L. Maschio, B. Kirtman, M. Rerat, R. Orlando, R. Dovesi, Ab initio analytical Raman intensities for periodic systems through a coupled perturbed Hartree-Fock/Kohn-Sham method in an atomic orbital basis. I. Theory, J. Chem. Phys. 139 (2013) 164101.
[13] L. Maschio, B. Kirtman, M. Rerat, R. Orlando, R. Dovesi, Ab initio analytical Raman intensities for periodic systems through a coupled perturbed Hartree-Fock/Kohn-Sham method in an atomic orbital basis. II. Validation and comparison with experiments, J. Chem. Phys. 139 (2013) 164102.
[14] M. Ferrero, M. Rerat, B. Kirtman, R. Dovesi, Calculation of first and second static hyperpolarizabilities of one- to three-dimensional periodic compounds. Implementation in the CRYSTAL code., J. Chem. Phys. 129 (2008) 244110.
[15] M. Ferrero, M. Rerat, R. Orlando, R. Dovesi, The calculation of static polarizabilities of 1-3D periodic compounds. The implementation in the CRYSTAL code, J. Comput. Chem. 29 (2008) 1450–1459.
[16] R. Dovesi, A. Erba, R. Orlando, C.M. Zicovich-Wilson, B. Civalleri, L. Maschio, M. Rerat, S. Casassa, J. Baima, S. Salustro, B. Kirtman, Quantum-mechanical condensed matter simulations with CRYSTAL, Wires Comput. Mol. Sci. 8 (2018) E1360.